Asian Journal of Civil Engineering (2020) 21:533–542
https://doi.org/10.1007/s42107-020-00226-2

ORIGINAL PAPER

Design guidelines of composite sections for concrete beams with profiled steel sheath encasement

Salah Taher[1,2] · Khaled Fawzy[1,3] · Nashwa Yossef[4]

Received: 22 August 2019 / Accepted: 20 January 2020 / Published online: 10 February 2020

Abstract

This investigation aims at establishing design guidelines for various limit states of concrete beams with profiled steel sheath encasement. This type is used when weldability is not suitable for thin sheets to form tubular sections. For concrete-filled profiled steel sheath (CFPS), three design criteria are considered in the proposed design guidelines: (1) ultimate limit state considering the imposed confinement of the profiled steel sheath encasement, (2) serviceability limit states for shored construction, and (3) sheath thickness to avoid local buckling. The partial shear connection allows for the design to depend on the bond's physical appearance of the concrete–steel interface. Verification of the proposed design procedures is carried out against two sets of previous investigations. The first set is a well-documented experimental program and a finite element analysis of several configurations of seventeen profiled sections. The other is a comparison with the predictions of selective international codes and analytical formulas for commonly used concrete-filled steel tubes (CFST). The results indicated very good predictions of the proposed guidelines and the suitability to capture the salient features of behavior of both CFPS and CFST.

Keywords Steel–concrete composites · Concrete-filled steel tubes · Profiled steel sheath sections · Confinement · Encasement

Introduction

Concrete-filled hollow steel sections gained popularity in multi-story buildings, especially in high seismic zones, bridges, space frames and offshore platforms due to its composite action and superior out-of-plane behavior (An et al. 2014). The inborn benefits of this system are derived from its structural conformations (Eurocode-4 2014). Hollow concrete steel sections will permit simple molding of in-fill concrete (Ghadge et al. 2018). Temporary formwork is not required for these sections to in-fill concrete because of the steel exploit as formwork in the erection period and a fortification in the working stage (Jaber et al. 2018). They are a great facility to manufacture and build admit of comparison conformist reinforced concrete, where accomplished labors are desirable to amend and twist complex configuration of reinforcement.

Although many approaches were adopted in different design codes, there is a lack of information, investigations, FE models and experimental results. That is why Soundararajan and Shanmugasundaram (2008) proposed a new approach in calculating the strength of a composite structure, which is commonly expressed in terms of the ultimate moment of resistance. The computation is based on these properties in full plastic stress distribution. Their analysis assumptions were as follows:

Salah Taher: On leave from Tanta University, Giza, 12411, Egypt.
Khaled Fawzy: On leave from Zagazig University, Zagagig, Egypt.

✉ Khaled Fawzy
Khaled_lashen1@yahoo.com

Salah Taher
salahftaher@yahoo.com

Nashwa Yossef
nashwa_abdeltawab@f-eng.tanta.edu.eg

1 Present Address: Delta University for Science and Technology, B.O. Box 44519, Zagazig, Sharkia, Egypt

2 Tanta University, Giza 12411, Egypt

3 Faculty of Engineering, Zagazig University, B.O. Box 44519, Zagazig, Sharkia, Egypt

4 Faculty of Engineering, Tanta University, Giza 12411, Egypt

- Initial plane sections remain plane after bending and normal to the neutral plane.
- All steel samples are at the yield stress equal to fsk = f y/ms (for steel) (ms _ = 1.0).
- Concrete in tension is ignored and the concrete above the neutral axis is under a uniform compression stress: fck = 0.67 fcu/1.5 = 0.4 fcu.

where fck is the characteristic strength of concrete, fcu is the characteristic 28-day cube of concrete, *fy* is the yield strength of structural steel and ms is the factor of safety.

By any manner of means, their usage has been restricted due to the absence of information about the extreme load capacity of these composite structures (Mol 2001). Concrete-filled steel sections take many forms (Wardenier et al. 1995). The most popular is using structural hollow section (SHS) taking the shape of a circle (CHS), rectangle (RHS), or others such as triangle, hexagon, octagon or flat oval. Such SHS may be either a hot-rolled section or welded plates taking the tubular form. The latter is widely known for concrete-filled steel tubes (CFST) as shown in Fig. 1a. Shallal (2018) investigated the flexural behavior of CFST, for square sections with dissimilar concrete strengths used to fill up the hollow of the steel units and concluded that for indistinguishable *D*/*t* and strength of concrete of square section beams ensued in developed load capabilities. However, in several applications, weldability may not be admissible for thin sheets and thus profiled steel sheath encasement is the alternative with the so-called concrete-filled profiled steel sheath sections (CFPS) as shown in Fig. 1a. Figure 1c illustrates the post-peak failure patterns of CFPS as reported through experiments and simulation.

There are several procedures to inaugurate the bond among the steel encasement and concrete (Hunaiti 2003) using either chemical bonding (Ghadge et al. 2018), mechanical techniques (by either mechanical interlock, frictional interlock, end anchorage by through-deck fixed studs or end anchorage by distortion of the ribs) (Eurocode-4 2014) or both. Several studies were conducted to investigate the composite action for specific sorts of concrete Shallal (2018), Virdi et al. (1980), Yousef et al. (2018), Zhang et al. (1994), Hunaiti (2003) found that using silica fume with steel fibers in reactive powder concrete mixture improved the bonds between the composite section components and thus increased the flexural beams resistance and decreased the deflection. The experimental work of Ghadge et al. (2018) demonstrated that the flexural strength of rectangular normal concrete composite section with mechanical bonding was higher than sections with a chemical bond of no-fines concrete or normal concrete.

CFST provides higher confinement than slotted CFPS due to its full encasement. Both have very acceptable performance under a flexural moment, related to conventional RC beams (Oehlers et al. 1994). In general, encasements bond with concrete is a proficient way to avoid intensely local buckling and to raise the strength of tube-shaped constructions with standard hot-rolled hollow sections (Patrick 1990). The strength of concrete is enhanced owing to the sideways confinement by the steel. Chen et al. (2018) introduced an original type of validator steel-encased RC beam to increase the bonding among steel and concrete and their accommodating performance. Donga et al. (2019) explored that the rubberized concrete was progressively compelling in postponing the untimely buckling failure of ordinary normal concrete with steel tube. Because of the possible segregation between RC and steel structure design, the design procedure of the CFST beam using the LFRD process recommended by the AISC "AISC-LRFD (1999)" is quite dissimilar from ACI 318-14 "ACI 318-14 (2014) and BS5400 "BS5400 (1979)".

Aravind and Mohammed (2017) discovered that compared to empty steel tubes, strength increase of 67.19%, 97.48%, and 114.84% was observed in normal CFST and CFST with sandblasting and CFST with diagonal shear connector beams, respectively. 17 rectangular concrete-filled steel tubular columns were tested by Qu et al. (2019) using a push-out test method to examine the interfacial bond behavior. All specimens were subjected to axial compression. Through a comparison of the numerical simulation results,

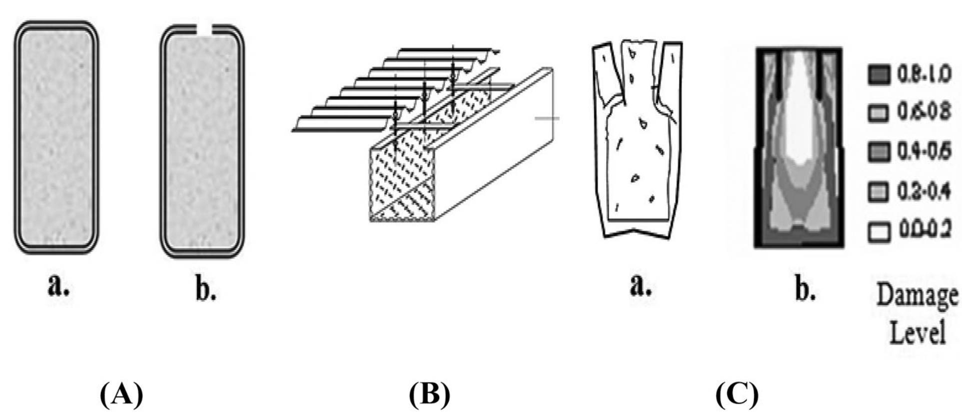

Fig. 1 **A** CFST (Han 2004); **B** CFPS: **a** slotted (Taher 2004a), **b** checkered steel plates (Chen et al. 2018); **C** Post-peak cracking pattern of CFPS: **a** experimental observations (Hossain 2003) and **b** finite element results for damage level (Taher 2004b)

formula calculation of the influence of interfacial damage on the axial compressive bearing capacity of a rectangular concrete-filled steel tubular column was discussed.

Several investigations focused on simulating the sophisticated composite action with a partial shear connection using nonlinear finite element (Al-Rodan and Al-Tarawnah 2003; Javed et al. 2017; Taher 2004a, b. Analytical models were developed based on particular presumptions for profiled composite beams (Han 2004; Hossain 2003; Javed et al. 2017; Oehlers et al. 1994; Taher 2004b). International codes led to diverse predictions of the ultimate capacity of the composite section (ACI 318-14 2014; AISC-LRFD 1999; BS5400 1979; Eurocode-4 2014; Permanent Code Committee 2018; Wardenier et al. 1995) due to the inconsistency in accounting for the relative slip of the composite components. Therefore, viable, rigorous, reliable yet simple design guidelines are needed for practitioner engineers. The current investigation basically derives design guidelines of composite sections for concrete beams with profiled steel sheath encasement.

Research significance

As the available literature lacks a unified design method for the flexural behavior of the square and rectangular concrete-filled profiled steel sheath (CFPS), therefore the main aim of this study is to establish an analytical procedure within limit states framework. For this purpose, available code provisions for CFST will be examined for particular case studies in terms of ultimate composite capacity, sheath buckling and serviceability to finally recommend the most suitable design for these sections (CFPS).

Existing flexural design formulae

Han (2004) model

As indicated by Han "Han (2004)", the ultimate moment of the CFST beam is given by:

$$M_u = f_{\mathrm{scy}} w_{\mathrm{scm}} \tag{1}$$

$$f_{\mathrm{scy}} = (1.18 + 0.85\,\zeta) f_{\mathrm{ck}} \tag{2}$$

$$w_{\mathrm{scm}} = B^2/6 \tag{3}$$

$$\zeta = A_s f_{\mathrm{yk}} / A_c f_{\mathrm{ck}} \tag{4}$$

$$\gamma_m = 1.04 + 0.48 \ln(\zeta + 0.1) \tag{5}$$

where is the moment capacity of the CFST beam, f_{scy} is the nominal yielding strength of the steel tube, W_{scm} is the section modulus of CFST cross-section,ξ is the constraining factor, and γ_{m} is the flexural strength index. However, Han's model cannot be used for ultra-high-strength concrete.

AISC-LRFD

The moment of the steel hollow section CFST beam according to AISC-LRFD (1999) may be estimated by:

$$M = Zf_y \tag{6}$$

where Z and f_y is the section modulus and the yield strength of steel tube, respectively.

CIDECT

The ultimate moment for CFST beams as indicated by the CIDECT Taher (2004a, b) can be defined as:

$$M_{u,CIDECT} = M_{ratio}\left[H^2 b - (H - 2t)^2(b - 2t)\right] f_y/4 \tag{7}$$

where M_{ratio} is a ratio of the bending capacity of the composite hollow section to that of the hollow section, H, t, and b is the depth, thickness, and width of composite section, respectively, f_y is the yielding stress.

Proposed model for ultimate limit state with partial composite action

Three design criteria are considered in the proposed design guidelines: (1) ultimate limit state considering the imposed confinement of the profiled steel sheath encasement, (2) serviceability limit states for shored construction and (3) sheath thickness to avoid local buckling. The partial shear connection is allowed for the design depending on the bond characteristics of the concrete–steel interface. The proposed procedures are elaborated hereafter.

Ultimate limit state

The analytical model developed hereafter is based on the ultimate limit states set, thus, considering the material safety factor. Partial as well as full connections are implemented in the proposed design procedure. The analysis is based on the following assumptions:

- Up to the furthest reaches of producing an interface stresses not surpassing the bond strength:
- The composite beam will display full interaction and there will be no slip over the steel–concrete interface.

- Similar strain dissemination will exist in sheeting and concrete with a nonpartisan pivot of both steel and concrete area,
- Nc, incidental to one another as appeared in Fig. 2.
- On the off chance, the greatest moment capacity is coming to without the interface bond force surpassing the interface bond strength, then the beam shows full composite activity or full collaboration.

Composite beam exhibits the partial interaction with an occurring slip if the interface bond force surpasses the interface bond strength (Patrick 1990; Virdi et al. 1980). Therefore, there will be a precarious change, *εsl* between the strain in sheeting and concrete as appeared in Fig. 2c. The situation of the neutral pivot for concrete Ncc is not quite the same as the steel sheeting Nss. As indicated by Oehlers et al. (1994), the slip strain should be consistent all through the depth of the beam that prompts a uniform slip at the ends. The flexural strength of the composite beam can be outlined by considering distribution of forces in the concrete and steel sections.

For the more general case of partial shear connection, Ncc ≠ Nss, and equilibrium of forces:

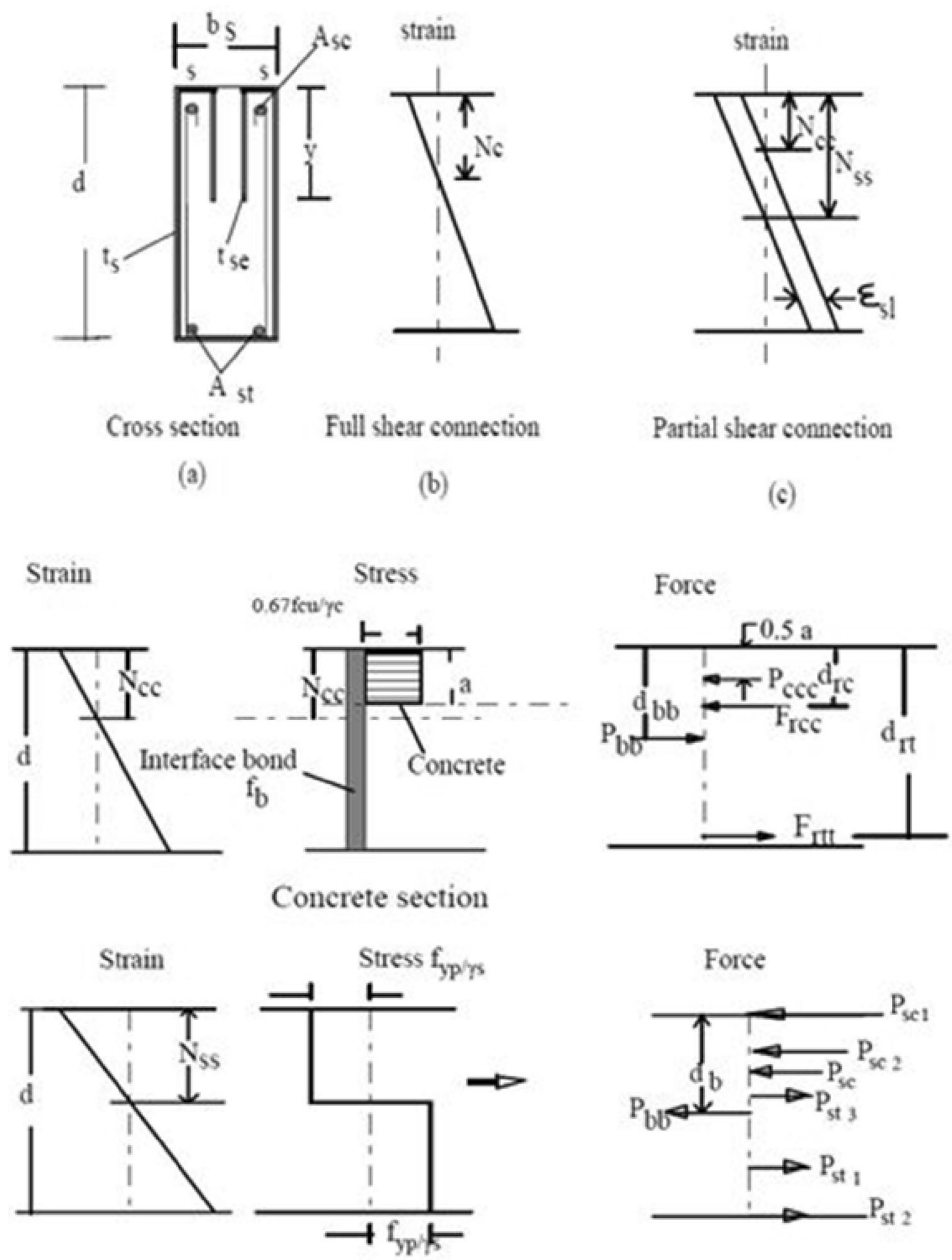

Fig. 2 Free body diagram, strain and equivalent stress blocks at the ultimate stage

$$F_{rcc} + P_{ccc} = F_{rtt} + P_{bb}$$
$$A_{sc}f_{rcc} + 0.67 f_{cu}/\gamma_c ab_c = P_{bb} + A_{st}f_{rtt} \quad (8)$$

where F_{rcc} is the compressive force in steel, P_{ccc} is the compressive force in concrete, P_{bb} is the force due to shear bond, F_{rtt} is the force in tensile steel, f_{rcc} is the stress in compressive steel and f_{rtt} is the stress tensile steel. Considering yield of both tension and compression reinforcements, the depth of concrete compression block a can be derived as:

$$a = \left(P_{bb} + F_{rtt} - F_{rcc}\right)/\left(0.67 f_{cu}b_c\right)$$
$$= \left(P_{bb} + A_{st}f_y/\gamma_s - A_{sc}f_y/\gamma_s\right)/\left(0.67 f_{cu}b_c\right) \quad (9)$$

in which f_y is the yield strength of the steel reinforcement, $b_c = b_s - 2t_s - 2t_{se}$ is the net width of concrete section. From strain compatibility, for yielded tensile and compressive steel:

$$\varepsilon_{sc} = \varepsilon_{cu}\left(N_{cc} - d_{rc}\right)/N_{cc} \geq \varepsilon_{sy}, \varepsilon_{st} = \varepsilon_{cu}\left(d_{rt} - N_{cc}\right)/N_{cc} \geq \varepsilon_{sy} \quad (10)$$

where ε_{sc} is the compression steel strain, ε_{st} is the tensile steel strain, ε_{cu} is the ultimate concrete strain = 0.003, ε_{sy} is the steel yield strain, d_{rc} is the compression steel depth and d_{rt} is the tensile steel depth. If the compression steel has not yielded, then Ncc is to be estimated based on actual stress–strain condition in the compression steel. The stress f_{rc} in the compression steel is:

$$f_{rc} = E_s\varepsilon_{sc} = E_s\varepsilon_{cu}\left(N_{cc} - d_{rc}\right)/N_{cc} \quad (11)$$

E_s is the reinforcing steel modulus of elasticity. The value of Ncc for the case when compression steel is not at yield can be derived by substituting for f_{rc} from Eqs. (8–11), leading to the following quadratic equation:

$$\left(0.67 f_{cu}/\gamma_c b_c\right) N_{cc}^2 + (A_{sc}E_s\varepsilon_s - A_{st}f_y/\gamma_s)N_{cc}$$
$$- P_{bb} - A_{sc}d_{rc}E_s\varepsilon_{cu} = 0 \quad (12)$$

The interface bond force of the beam can be expressed as:

$$P_{bb} = \sum\nolimits_0 f_{bb}x \quad (13)$$

where $\sum_o$ is the cross-sectional perimeter of steel sheeting in contact with concrete, x is the distance from the support to the critical section in flexure and f_{bb} is the shear bond stress at the interface. Considering the case of welded extension extending below the neutral axis ($y > N_{ss}$) and from the equilibrium of steel section:

$$P_{bb} + P_{scc} + P_{sc1} + P_{sc2} = P_{st1} + P_{st2} + P_{st3}$$
$$P_{bb} + 2\left(f_{yp}/\gamma_{sp}\right)N_{ss}t_s + 2\left(f_{yp}/\gamma_{sp}\right)N_{ss}t_{se} + 2\left(f_{yp}/\gamma_{sp}\right)t_s s =$$
$$\Rightarrow 2\left(d - N_{ss}\right)\left(f_{yp}/\gamma_{sp}\right)t_s + b_s t_s\left(f_{yp}/\gamma_{sp}\right) + 2\left(y - N_{ss}\right)t_{se}f_{yp}/\gamma_{sp} \quad (14)$$

where P_{bb} is the bond force, P_{sc}, P_{sc1} and P_{sc2} are the compressive forces in the web, top and welded extension steel above the neutral axis, respectively; P_{st1}, P_{st2} and P_{st3} are the tensile force in the web, bottom and welded extension steel below the neutral axis, respectively, and f_{yp} is the yield stress of steel plate:

$$N_{ss} = \left(\left(f_{yp}/\gamma_{sp}\right) t_s\left(2d + b_s - 2s\right) + 2y\,t_{se}\left(\left(f_{yp}/\gamma_{sp}\right) - P_{bb}\right)\right)/$$
$$4\left(t_s\left(f_{yp}/\gamma_{sp}\right) + t_{se}\left(f_{yp}/\gamma_{sp}\right)\right) \quad (15)$$

Considering the yielding of steel, the depth of the neutral axis N_{ss} for the case of no welded extension ($y = 0$) can be derived as:

$$N_{ss} = \left(\left(f_{yp}/\gamma_{sp}\right)t_s\left(2d + b_s - 2s\right) - P_{bb}\right)/4\left(t_s f_{yp}/\gamma_{sp}\right) \quad (16)$$

Taking moment of all the forces about the top fiber of the beam, the moment capacity, M_u with doubly reinforced concrete core considering partial interaction can be determined from the expression:

$$M_u = t_s f_{yp}/\gamma_{sp}\left(d^2 + d\,b_s - 2N_{ss}^2\right) + t_{se}f_{yp}/\gamma_{sp}\left(y^2 - 2N_{ss}^2\right)$$
$$+ f_{rtt}A_{st}d_{rt} - f_{rcc}A_{sc}d_{rc} - 0.67\,a^2 b_c f_{cu}/\gamma_c \quad (17)$$

For plain concrete core with welded extension ($y > N_{ss}$), the equation reduces to:

$$M_u = t_s f_{yp}/\gamma_{sp}\left(d^2 + d\,b_s - 2N_{ss}^2\right) + t_{se}f_{yp}/\gamma_{sp}\left(y^2 - 2N_{ss}^2\right)$$
$$+ f_{rtt} - 0.67\,a^2 b_c f_{cu}/\gamma_c \quad (18)$$

and for plain concrete without welded extension ($y = 0$),

$$M_u = t_s f_{yp}/\gamma_{sp}\left(d^2 + d\,b_s - 2N_{ss}^2\right) - 0.67\,a^2 b_c f_{cu}/\gamma_c \quad (19)$$

On the other hand, for plain concrete with welded extension not extending below the neutral axis ($y < N_{ss}$),

$$M_u = t_s f_{yp}/\gamma_{sp}\left(d^2 + db_s - 2N_{ss}^2\right) - t_{se}f_{yp}/\gamma_{sp}\left(y^2\right) - 0.67\,a^2 b_c f_{cu}/\gamma_c \quad (20)$$

For doubly reinforced with welded extension not extending below the neutral axis ($y < N_{ss}$),

$$M_u = t_s f_{yp}/\gamma_{sp}\left(d^2 + db_s - 2N_{ss}^2\right) + t_{se}f_{yp}/\gamma_{sp}\left(y^2\right)$$
$$+ f_{rtt}A_{st}d_{rt} - f_{rcc}A_{sc}d_{rc} - 0.67\,a^2 b_c f_{cu}/\gamma_c \quad (21)$$

Serviceability limit states

Estimation of the short-term and long-term deflection of the composite section depends on the shoring condition. For shored construction, the flexural stiffness is the stiffness of the entire composite section for dead, live, shrinkage, thermal, creep and other influences. On the other hand, for unshored construction, the deflection due to own weight is calculated based on the steel section stiffness, while the other load and live loads are calculated based on the stiffness of the composite section. The formulations for the flexural stiffness of the composite sections, K_c, in various codes are expressed in following general form:

$$K_c = E_s I_s + c E_c I_c \tag{22}$$

in which E_s and E_c *are* young's modulus of steel and concrete, respectively, while I_s and I_c are moments of inertia of the steel and concrete sections, respectively. χ is a factor related to the modular ration, where

$$\text{For ACI} - 318\text{//ACI } 318 - 14(2014)\text{//}\chi = 0.2 \tag{22-a}$$

$$\text{For AISC} - \text{LRFD//AISC} - \text{LRFD } (1999)\text{//}\chi = 0.8 \tag{22-b}$$

$$\text{For BS5400 //BS5400 (1979)//}\chi = 1.0 \tag{22-c}$$

$$\text{For Eurocode 4 //Eurocode} - 4(2014)\text{//}\chi = 0.6 \tag{22-d}$$

For many practical purposes of concrete-filled sections, the last ratio was found to yield reasonable estimations of the deflection (Han 2004; Jaber et al. 2018; Javed et al. 2017).

On the other hand, the cracking limit state is difficult to be visualized experimentally because of the existence of the encasement. However, the routine procedures may be considered to ensure the integrity of the sectional behavior. It should be kept in mind that the monitored behavior by Zhang et al. (1994) emphasizes on the essence of modeling micro-cracking and the shear connection of the composite element as such.

Buckling considerations

To safeguard section against instability, buckling stress of steel sheath should be maintained greater than the yield strength that means that buckling commences after yielding. The general form used by many codes for determining the effective width (b_{ef}) of a steel plate is given by Oehlers et al. (1994):

$$b_{\text{ef}}/b_s = \sqrt{(\sigma_{01}/\sigma_y)} \tag{23}$$

where b_s is the steel plate width; α is the factor to account for residual stresses and initial imperfections; σ_{o1} is the local buckling stress; σ_y is the steel yield stress.

To prevent the early buckling failure of steel hollow specimens, the allowable d/t_s ratio of the steel hollow sections may be taken as specified in EC4 as given below by the present terminology:

$$d/t_s \leq 52\sqrt{(235/f_{yp})} \tag{24}$$

where f_{yp} is the steel yield stress in N/mm^2, d is the depth of the section, t_s is the thickness of the section.

Model predictions for CFPS

Seventeen test specimens made of normal concrete in the well-reported comprehensive experimental program conducted by Hossain (2003) to study the performance of concrete-filled thin-walled composite beams are considered in this study. The test specimens were fabricated with varying geometric, material and interface connection parameters. Based on the geometric and mode of connections shown in Fig. 3, the beams were classified into open (SOS), welded extension (EWE), welded extension with the rod (VWER), braced (BS), closed (SCS), and (e) RC filled. The three aeries AA, BB, and CC as designated in the experimental program were considered in the analysis under four-point loading as listed in Table 1.

Beams A11 and A22 were considered to study the performance of comparatively slender SOS beams (L = 1500 mm) with normal (NC). In series BB, a total of seven beams consisting of two SOS, two SCS, one BS, two EWE (L = 600 mm) were tested to study the effect of connections enhancing the sheet–concrete interaction. A total of eight beams in series C, designated as CB, consisting of EWE, VWER and CRC (L = 990 mm; f_y = 455 MPa) are shown in Fig. 3. EWE beams had 0.48 mm welded extension plates tag welded at 150 mm, while VWER beams were added with additional restraint to enhance the interaction between the sheeting and concrete with 6 mm rods welded to the bottom of the extension plate at 150 mm. EWE and VWER beams had welded extension up to about one quarter and half of the depth of the beam with 40 mm diameter punching holes in the extension plates. RC beam CB7 was provided with only four 6 mm rods longitudinal reinforcements, whereas CB8 was similar but with stirrups 6 mm @150 mm.

The analysis of the case studies indicated the adequacy of the selected steel sheathing against local buckling. In addition, Fig. 4 depicts the close agreement of the predicated ultimate capacity for flexure with the reported experimental data (Hossain 2003). In the analysis, several assumed bond stresses have been examined (f_b = 0.1, 0.2, 0.3 and 0.4 N/mm^2) and the best agreement was obtained for the highest bond stress. This may be attributable to using volcanic admixtures of an expansive nature in the experimental work and thus exhibited the highest contact between concrete and the steel sheath. Figure 5 illustrates the effect of the bond stress on the ultimate flexural capacity of the several beams. The highest value has been

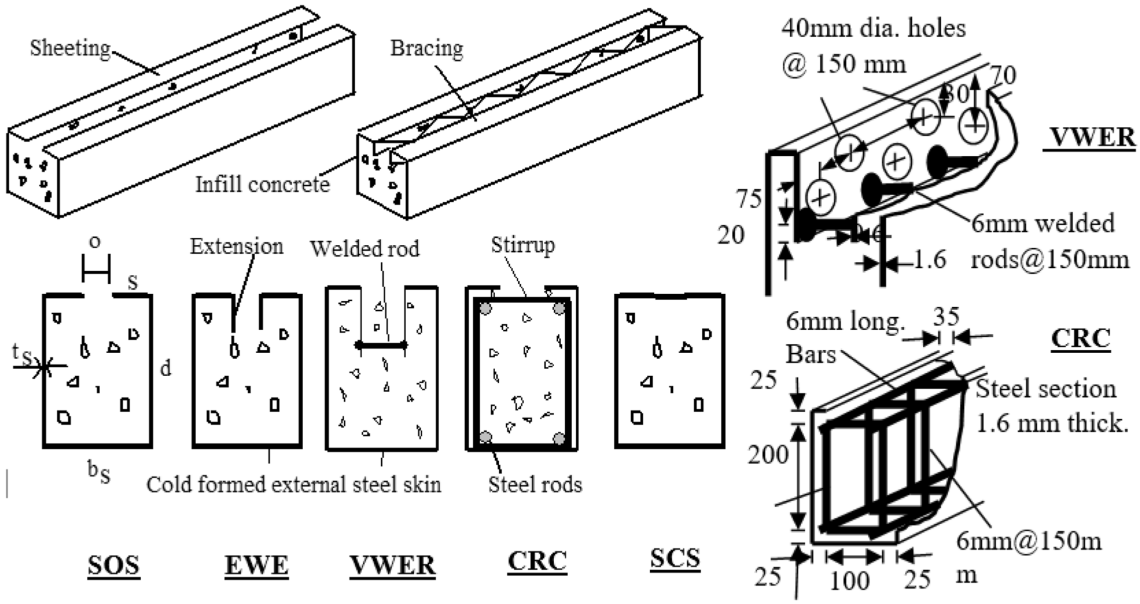

Fig. 3 Description of composite beams considered as study cases (Hossain 2003)

Table 1 Details of case studies considered in the verification "Hossain (2003)"

Series	Beam	Strength		Dimensions (mm)					Configuration[a]	f_b	P_u
		f'_c (MPa)	f_{yp} (MPa)	b_s	d	o	y	ts		(N/mm^2)	(kN)
AA	A11	21	375	100	100	20	0	3.2	SOS, NNMR, NNS	0.44	66.5
	A22	21	350	50	100	10	0	2.3	SOS, NNMR, NNS	0.25	65.0
BB	B13Inc	21	375	100	100	20	0	3.2	SOS, NNMR, NNS	0.73	111.0
	B13IInc	21	375	100	100	0	0	3.2	SCS, NNMR, NNS	0.48	158.0
	B14IInc	21	350	50	100	0	0	2.3	SCS, NNMR, NNS	0.38	125.0
	B13d/4nc	21	375	100	100	20	25	3.2	EWE, NNMR, NNS	0.36	71.0
	B13d/2nc	21	375	100	100	20	50	3.2	EWE, NNMR, NNS	0.56	128.0
	B14Inc	33.3	350	50	100	10	0	2.3	SOS, NNMR, NNS	0.33	103.0
	B14IIInc	33.3	350	50	100	10	0	2.3	BS, NNMR, NNS	0.44	84.0
CC	CB1	21	257	150	250	35	50	1.6	SOS, NNMR, NNS	0.59	140.0
	CB2	21	257	150	250	35	62.5	1.6	EWE, NNMR, NNS	0.42	144.0
	CB3	21	257	150	250	35	62.5	1.6	VWER, NNMR, NNS	0.42	170.0
	CB4	21	257	150	250	35	62.5	1.6	EWE, NNMR, NNS	0.49	147.0
	CB5	33	275	150	250	35	125	1.6	EWE, NNMR, NNS	0.42	177.0
	CB6	33	275	150	250	35	125	1.6	VWER, NNMR, NNS	0.42	235.0
	CB7	33	275	150	250	35	0	1.6	SOS, MMR, NNS	0.70	198.0
	CB8	33	275	150	250	35	0	1.6	CRC, MMR, S	0.70	225.0

f'_c is the concrete cylinder strength, f_{yp} is the yield stress of the steel sheath, f_b is the concrete–steel sheath bond stress, P_u is the ultimate load
[a]MMR, NNMR, NNS: with main reinforcement, no main reinforcement, no stirrup, respectively

considered as the reference for each specimen individually. Although slightly different, the ultimate flexural capacity is noted to be proportional to the bond stress.

To calibrate the predictions of CFST, Table 2 lists the close agreement of the results obtained by the proposed procedure with the experimental data of specimens B3IInc and B4IInc and in a better agreement than other design formulae. The selected formulas are the widely used design methods after AISC-LRFD (1999), Han (2004)" and CIDECT Wardenier et al. (1995). It can be noted that these

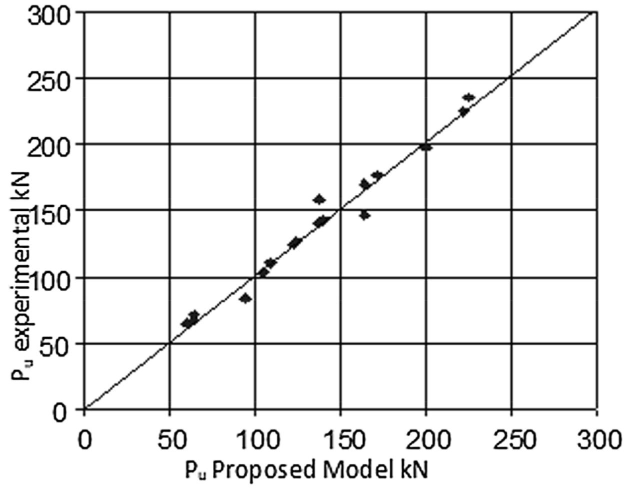

Fig. 4 Comparison of the predictions by the proposed guidelines and the reported experimental Hossain (2003) ultimate load capacity

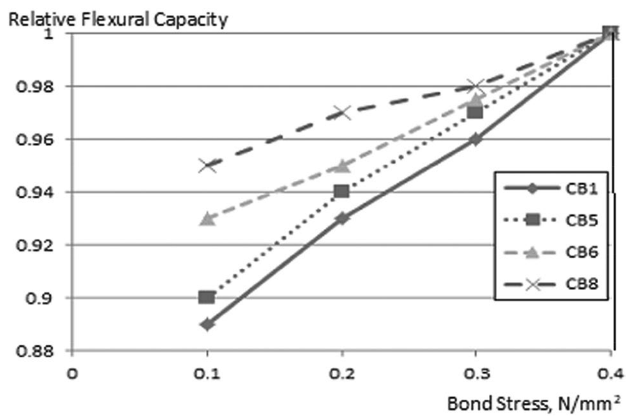

Fig. 5 Effect of bond stress on the overall flexural capacity of CFPS

design methods had higher discrepancies compared with the predictions of the proposed guidelines. In another aspect of service stage, Fig. 6 illustrated the reasonable estimation of the proposed design procedure for selective CFPS specimens.

For many practical purposes of concrete-filled sections, the last ratio was found to yield reasonable estimations of the defection (Han 2004; Jaber et al. 2018; Javed et al. 2017). On the other hand, the cracking limit state is difficult to be visualized experimentally because of the existence of the

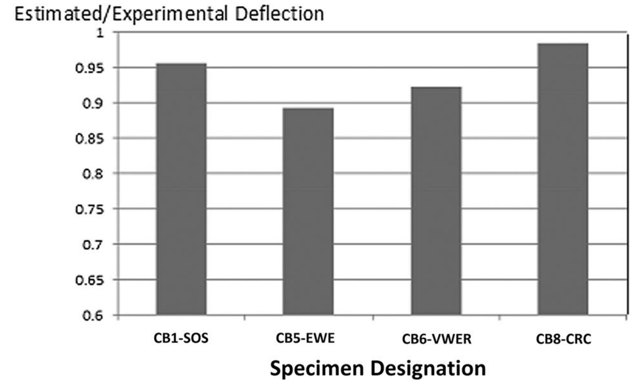

Fig. 6 Comparison of the predictions by the proposed guidelines and the reported experimental Hossain (2003) for deflection

encasement. However, the routine procedure may be considered to ensure the integrity of the sectional behavior. It should be kept in mind that the monitored behavior by Zhang et al. (1994) put emphasis on the essence of modeling micro-cracking and the shear connection of the composite element as such.

Model predictions for CFST

For calibration, nine square CFST sections were examined against the finite element (FE) model results Javed et al. (2017) and the proposed model versus particular codes' predictions. The estimations are listed in Table 3 that demonstrates the agreement of the results obtained by the proposed procedure closest to capacity reduction factors of the ratio of moment capacitates from FE Javed model results (Javed et al. 2017). On the basic behavior of square CFST beams filled with concrete with different parameters including depth-to-thickness ratio, concrete compressive strengths and steel yield strengths. According to the relative variation that shown in Table 3, the analytical guidelines and Han's model (2004) thoroughly proved its agreement with well-documented case studies better than AISC-LRFD (1999), and CIDECT Wardenier et al. (1995).

Table 3 compares CFST specimens against selective design formulae (AISC-LRFD 1999; Han 2004; Wardenier et al. 1995).

Table 2 Comparison of particular specimens against selective design formulae "AISC-LRFD (1999), Han (2004), Wardenier et al. (1995)"

Beam	P_{exp} (kN)	$P_{Present}$ (kN)	$P_{Present}/P_{exp}$	$P_{AISC\text{-}LRFD}$ (kN)	$P_{AISC\text{-}LRFD}/P_{exp}$	P_{CIDECT} (kN)	P_{CIDECT}/P_{exp}	P_{Han} (kN)	P_{Han}/P_{exp}
B13IInc	158.0	155.0	0.981	180	1.139	168.7	1.067	181.35	1.147
B14IInc	125.0	123.0	0.984	80.4	0.785	75.9	0.736	92.19	0.895

Table 3 Comparison of CFST specimens against selective design formulae "AISC-LRFD (1999), Han (2004), Wardenier et al. (1995)"

Cross-section (mm)	Thickness (Mm)	Yield strength (MPa)	Compressive strength (MPa)	Mu $_{FE}$ (kN m)	Mu Present (kN m)	$Mu_{AISC-LRFD}$ (kN m)	Mu_{CIDECT} (kN m)	Mu_{Han} (kN m)
80×80	3	410	60	13.75	13.75	10.57	11.83	13.11
80×80	3	500	60	18.15	15.45	12.89	14.23	15.55
80×80	3	600	60	23.10	18.45	15.47	16.83	18.27
80 × 80	2.5	345	60	13.20	9.00	7.56	8.55	9.59
80 × 80	2.5	345	80	13.20	9.15	7.56	8.70	10.20
80 × 80	2.5	345	100	14.85	9.28	7.56	8.78	10.73
80 × 80	2.5	345	30	11.55	8.77	7.56	8.27	8.58
80 × 80	3	345	30	13.20	10.58	8.89	9.61	10.37
80 x 80	4	345	30	14.85	14.28	11.41	12.19	14.33
Sum				136.95	108.71	89.47	98.99	110.73
Relative variation = Mu/Mu $_{FE}$				1.0	0.793793	0.653304	0.722819	0.808543

Conclusions

Limit states design guidelines have been established for various concrete beams encased by profiled steel sheath (CFPS). From the present research, the following conclusions may be drawn:

- Analytical guidelines have been developed for the flexural capacity of concrete-filled profiled steel sheath (CFPS) beams with partial shear connection controlling by the ultimate limit state, serviceability limit states and stability limit state to control sheath buckling. The influential parameters were found to be *d/t_s ratio*, yield strength of steel, and compressive strength of concrete, the imposed bond due to sheath confinement, and serviceability variables for shored construction.
- Verification of the proposed design guidelines for (CFPS) is carried out against previous well-documented experimental and finite element investigations along with selective international codes for concrete-filled steel tubes (CFST).
- The results indicated very good predictions of the proposed guidelines and the suitability to capture the salient features of the behavior of both CFPS and CFST.

Compliance with ethical standards

Conflict of interest On behalf of all authors, the corresponding author states that there is no conflict of interest.

References

ACI 318-14. (2014). *Building code requirements for structural concrete*. Farmington: Detroit: American Concrete Institute.

AISC-LRFD. (1999). *Load and resistance factor design specification for structural steel buildings* (2nd ed.). Chicago: American Institute of Steel Construction (AISC).

Al-Rodan, A., & Al-Tarawnah, S. (2003). FE analysis of the flexural behavior of rectangular tubular sections filled with high-strength concrete. *Emirates Journal for Engineering Research, 8*(1), 71–77.

An, Y. F., Han, L. H., & Roeder, C. (2014). flexural performance of concrete-encased concrete filled steel tubes. *Magazine of Concrete Research, 66*(5), 249–267. https://doi.org/10.1680/macr.13.00268.

Aravind, S., & Mohammed, Rafi D. (2017). A study on flexural behaviour of concrete filled steel tubes. *IJSRST, 3*(6), 621–626.

BS5400. (1979). *Concrete and composite bridges; code of practice for design of composite bridges*. London: British Standards Institution.

Chen, L., Li, S., Zhang, H., & Wu, X. (2018). Experimental study on mechanical performance of checkered steel-encased concrete composite beam. *Journal of Constructional Steel Research, 143,* 223–232. https://doi.org/10.1016/j.jcsr.2017.12.021.

Donga, M., Elchalakania, M., Karrecha, A., Hassanein, M. F., Xiec, T., & Yangd, B. (2019). Behaviour and design of rubberised concrete filled steel tubes under combined loading conditions. *Thin-Walled Structures, 139,* 24–38. https://doi.org/10.1016/j.tws.2019.02.031.

Eurocode-4. (2014). *Design of composite steel and concrete structures, general rule and rules for buildings*. London: British Standards Institution.

Ghadge, M., Galatage, A., & Bavdhankar, S. (2018). Performance of hollow sections with and without infill under compression and flexure. *International Journal of Engineering Science Invention (IJESI), 7*(2), 67–80.

Han, L. H. (2004). Flexural behaviour of concrete-filled steel tubes. *Journal of Construction Steel Research, 60*(2), 313–337. https://doi.org/10.1016/j.jcsr.2003.08.009.

Hossain, K. M. A. (2003). "Experimental and theoretical behavior of thin walled composite filled beams". *Elect Journal of the Structural Engineering, 3,* 117–139.

Hunaiti, Y. M. (2003). Aging effect on bond strength in composite sections. *Journal of Materials in Civil Engineering ASCE, 6*(4), 469–473.

Jaber, M. H., Al-Salim, N. H., & Hassan, R. F. (2018). flexural behavior of hollow rectangular steel (HRS) section beams filled with reactive powder concrete. *International Journal of Civil Engineering and Technology (IJCIET), 9*(5), 1177–1187.

Javed, M. F. Ramli, Rehman, N. H., & Khan, N. B. (2017). Finite element analysis on the structural behaviour of square CFST. *International Technical Postgraduate Conference Material Science and Engineering*. https://doi.org/10.1088/1757-899X/210/1/012018.

Mol. L. T. (2001). "Behaviour of Thin Walled Composite Structural Elements" *MPhil Thesis, Department of Civil Engineering, University of Technology*, PMB, Lae, Papua New Guinea.

Oehlers, D. J., Wright, H. D., & Burnet, M. J. (1994). Flexural Strength of Profiled Beams. *Journal of Structural Engineering, 120*(2), 378–393.

Patrick, M. (1990). A new partial shear connection strength model for composite slabs. *Journal of the Australian Institute of Steel Construction, 24*(3), 2–17.

Permanent Code Committee. (2018). "Egyptian code of practice for design and execution of reinforced concrete structures, ECP203" Ministry of Housing and Infrastructures, Egypt.

Qu, X., Huang, F., Sun, G., Liu, Q., & Wang, H. (2019). Axial compressive behaviour of concrete-filled steel tubular columns with interfacial damage. *Advances in Structural Engineering*. https://doi.org/10.1177/1369433219891639.

Shallal M. A. (2018). "Flexural behavior of concrete-filled steel tubular beam", *International Conference on Advances in Sustainable Engineering and Applications (ICASEA)*, Waist University, Kut, Iraq. 978-1-5386-3540-7/18/31.00$©2018 IEEE.

Soundararajan, A., & Shanmugasundaram, K. (2008). Flexural behaviour of concrete-filled steel hollow sections beams. *Journal of Civil Engineering and Management, 14*(2), 107–114. https://doi.org/10.3846/1392-3730.2008.14.5.

Taher S. F. (2004a). "Progressive-fracturing concrete damage model for thin walled composite filled beams" *IC-SGECT'04, International Conference on Structural & Geotechnical Engineering and Construction Technology*, Mansoura, Egypt.

Taher, S. F. (2004b). composite shear connection in partially steel sheath encased concrete filled beams. *Science Bulletin, 39*(2), 41–58.

Virdi, K. S.& Dowling, P. J. (1980). Bond strength in concrete-filled steel tubes *IABSE Periodica 3*, Proceeding, P-33/80, 125-139.

Wardenier, J., Dutta, D., Yeomans, N., Packer, A., & Bucak, O. (1995). *Design guide for structural hollow sections in mechanical applications*. Köln: Verlag TÜV Rheinland, CIDECT.

Yousef, N., & Taher, S. F. (2018). Cost optimization of composite floor systems with castellated steel beams. *Practice Periodical on Structural Design and Construction ASCE*. https://doi.org/10.1061/(ASCE)SC.1943-5576.0000409.

Zhang, J. Q., & Brahmachari, K. (1994). *Flexural behavior of rectangular tubular sections filled with fibrous high strength concrete tubular structures VI* (pp. 247–254). Holland: Rotterdam.